

# The recent history of the X-ray absorber in NGC 3516

M. Guainazzi<sup>1,2</sup>, W. Marshall<sup>2,3</sup>, A. N. Parmar<sup>2</sup>

<sup>1</sup> *XMM-Newton SOC, VILSPA ESA, Apartado 50727, E-28080 Madrid, Spain*

<sup>2</sup> *Astrophysics Division, Space Science Department of ESA, ESTEC, Postbus 299, NL-2200 AG Noordwijk, The Netherlands*

<sup>3</sup> *Leicester University, Leicester LE1 7RH, United Kingdom*

25 November 2018

## ABSTRACT

We present two BeppoSAX observations of the bright Seyfert 1 galaxy NGC 3516, performed four months apart (late 1996/early 1997). The earlier spectrum is considerably weaker and harder in the whole 0.1–50 keV energy range. In addition, the warm absorber oxygen features, which were already observed with ROSAT (Mathur et al. 1997) and ASCA (Kriss et al. 1996), are much less pronounced. The most straightforward explanation is that in 1996 November NGC 3516 was being seen through a substantial ( $N_{\text{H}} \simeq 10^{22} \text{ cm}^{-2}$ ) column of cold material. This is the first confirmation with modern instrumentation that NGC 3516 indeed undergoes phases of strong cold X-ray absorption. We speculate that these intervals may be connected to the onset of the remarkably variable UV absorption system, making NGC 3516 the best known example of low-luminosity Broad Absorption Line (BAL) quasar. The absorbing matter could be provided by clouds ablated from the rim of the circumnuclear molecular torus, seen at a rather high inclination angle.

**Key words:** Galaxies: individual: NGC3516 – Galaxies: nuclei – Galaxies: Seyfert - X-rays: general

## 1 INTRODUCTION

The X-ray spectra of type 1 Seyferts do not show substantial amounts of photoelectric absorption by neutral matter (Mushotzky 1982; Turner & Pounds 1989). This is consistent with a scenario where these objects are seen along the axis of a dusty molecular torus surrounding the nucleus (Antonucci & Miller 1985; Antonucci 1993). However, about 50% of Seyfert 1 galaxies exhibit soft X-ray features due to photoelectric absorption by highly ionized matter, mostly He- and H-like oxygen (Reynolds 1997; George et al. 1998a). The physical condition of the absorber and its location are still matter of debate. The existence of a copious source of high-energy photons in Active Galactic Nuclei (AGN) suggests that the ionization structure of the absorbing material could be driven by the same non-thermal nuclear high-energy continuum that we observe. However, in several cases (and, most noticeably, in the best studied ones: MCG-6-30-15, Fabian et al. 1994; Reynolds et al. 1995; NGC 4051, McHardy et al. 1995; Guainazzi et al. 1996), the variability patterns on short (*i.e.*: hours) and medium (*i.e.*: days/weeks) timescales suggest a more complex picture than a single-zone medium in thermal and ionization equilibrium with the primary (nuclear) continuum. A physically

stratified medium (Otani et al. 1996; George et al. 1998b) or models of non-equilibrium and/or collisional excitation (Nicastro et al. 1999a) are two alternative possibilities. The high-resolution observations to be provided by the grating systems on-board *Chandra* and XMM, will allow the ionization structure of the absorbing regions to be studied in detail.

However, variability studies are still an important tool in helping determine the location of the absorbing material. These studies generally rely on sparse and mostly episodic monitoring campaigns. The original post-ROSAT suggestion that the warm absorber is coincident or co-located with the Broad Line Region (Mushotzky et al. 1993) is consistent with current observational evidence (Guainazzi et al. 1996; Fabian et al. 1994; George et al. 1998a), and is discussed in detail for the case of NGC 3516 by Kolman et al. (1993), who derive a loose constraint on the distance to the absorber of 0.01–9 pc.

Recently, Boller et al. (1997) and Guainazzi et al. (1998) have speculated that the dramatic variability observed in a few Narrow Line Seyfert Galaxies may be due to the interposition of randomly distributed “bricks” of material with  $N_{\text{H}} \gtrsim 10^{22} \text{ cm}^{-2}$  along the line of sight. The sampling of this variability and the available spectral resolution is gen-

erally not good enough to exclude alternative mechanisms, and it is still not clear how general this phenomenology is in Seyfert galaxies as a class.

This *paper* presents two recent BeppoSAX observations of the nearby ( $z = 0.0088$ ) Seyfert 1 galaxy NGC 3516, which reveal new interesting features, relevant to the above issues. NGC 3516, being one of the brightest Seyfert 1s in the X-ray sky, has been extensively studied by all the major X-ray observatories. Low-resolution, bandwidth-limited observations in the 1980s suggested an extreme variability, more pronounced in the soft X-ray band. Two observations with the Imaging Proportional Counter on-board *Einstein* showed an increase by a factor of 5 of the 0.2–4.0 keV flux, accompanied by a large change in spectral shape (the lower the flux, the flatter the spectrum; Kruper et al. 1990). Monitoring with the Monitor Proportional Counter (MPC) on-board *Einstein* and with EXOSAT (Ghosh & Soundararajaperumal 1991) revealed strong and highly variable ( $0.5\text{--}2 \times 10^{23} \text{ cm}^{-3}$ ) photoelectric absorption. However, with the advent of the moderate energy resolution provided by the ROSAT Position Sensitive Proportional Counter and by ASCA, it has been possible to identify NGC 3516 as one of the “warm absorbed” Seyfert 1s. Comparison of the ASCA observations with detailed photoionization models suggests the presence of a complex multi-zone warm absorber, with a broad (*i.e.* almost one order of magnitude) range of ionization parameters and column densities ( $N_{\text{H,warm}} : 0.7\text{--}1.5 \times 10^{22} \text{ cm}^{-2}$ ; Kriss et al. 1996). Mathur et al. (1997) investigated the possible connection between the X-ray absorber and the strong, broad and variable UV lines (Voit, Shull & Begelman 1987; Walter et al. 1990; Kolman et al. 1993; Koraktar et al. 1996), and suggested that the absorbers are indeed one and the same outflowing system. A quasi-simultaneous *Ginga* and HST observation of NGC 3516 suggested the presence of significant amount of cold photoelectric absorption ( $N_{\text{H,cold}} \equiv N_{\text{H}} \sim 4 \times 10^{22} \text{ cm}^{-2}$ ) as well as the warm absorber. The limited soft X-ray coverage of the *Ginga* Large Array Counter did not allow an unambiguous spectral deconvolution so the different contribution to the complex absorption could not be separated. George et al. (1998a) comment that the rather flat ( $\Gamma \simeq 1.5$ ) spectral index and the substantial amount of neutral absorption measured by *Einstein*, EXOSAT and *Ginga* were (“undoubtedly”) due to an incorrect modeling of ionized features with neutral gas.

The observations performed by BeppoSAX (Boella et al. 1997a) allows for the first time the spectrum of NGC 3516 to be simultaneously measured over more than three decades in X-ray energy (0.1–200 keV), thus ensuring the best spectral deconvolution so far. Although the energy resolution of the BeppoSAX instruments is insufficient to allow high-resolution spectroscopy of the soft X-ray features, drastic changes in the properties of the X-ray absorber are clearly evident between the two observations performed about four months apart. This is the main focus of this *paper*, together with the presentation of the still unpublished X-ray broadband spectrum. Sect. 2 describes the observations and the reduction procedures. The presentation of the BeppoSAX results is dealt with in Sects. 3 and 4 and our findings are discussed in Sect. 5.

## 2 OBSERVATION AND DATA REDUCTION

The Italian-Dutch satellite BeppoSAX carries four co-aligned Narrow Field Instruments. Two imaging gas scintillation proportional counters: the Low Energy Concentrator Spectrometer (LECS, 0.1–10 keV, Parmar et al. 1997) and the Medium Energy Concentrator Spectrometer (MECS, 1.8–10.5 keV, Boella et al. 1997b). The other two instruments have non-imaging detectors and use rocking collimators to monitor the background: the High Pressure Gas Scintillator Proportional Counter (HPGSPC, 4–120 keV, Manzo et al. 1997) and the Phoswich Detector System (PDS, 13–200 keV, Frontera et al. 1997). The HPGSPC is optimized for spectroscopy of bright sources with good energy resolution, while the PDS possesses an unprecedented sensitivity in its energy bandpass.

BeppoSAX observed NGC 3516 twice: on 1996 November 8 between 02:34 and 22:52 UTC, and between 1997 March 11 06:06 and March 12 01:01 UTC. Exposure times for each instrument are shown in Tab. 1, together with the observed background-subtracted count rates in the 0.1–2 keV, 2–10 keV and 15–200 keV energy ranges. Data were telemetered in direct modes for all instruments, which provide full information about the arrival time, energy, burst length/rise time (RT) and, when available, position for each photon.

In this *paper* data from all the scientific payload BeppoSAX instruments are presented. Standard reduction procedures and screening criteria have been adopted to produce linearized and equalized event files. In particular, time intervals have been excluded from the scientific product accumulation when the angle between the pointing direction and the Earth’s limb was  $< 5^\circ$  and the momentum associated to Geomagnetic Cutoff Rigidity was  $> 6 \text{ GeV/c}$  as the satellite passed through the South Atlantic Geomagnetic Anomaly (SAGA).

The PDS data have been further screened by eliminating 5 minutes after each SAGA passage to avoid gain instabilities due to the recovery to the nominal voltage value after instrumental switch-on. The RT selection has been performed using crystal temperature dependent thresholds (instead of the fixed thresholds in the standard processing). Spectra of the imaging instruments have been extracted from circular regions of radius  $8'$  around the centroid of the source for the LECS and MECS. Background subtraction was performed using spectra extracted from blank sky exposures in the same region as the source. The HPGSPC and PDS background-subtracted spectra and light curves were produced by subtraction of the “off-” from the “on-source” data. The spectra have been rebinned in order to oversample the Full-Width Half-Maximum of the energy resolution by a factor not greater than 3 and to have at least 20 counts per spectral channel, to ensure the applicability of the  $\chi^2$  test. Uncertainties are quoted at 90% level of confidence for one interesting parameters ( $\Delta\chi^2 = 2.71$ ; Lamp-ton et al. 1976) and energies are in the source rest frame;  $H_0 = 50 \text{ km s}^{-1} \text{ Mpc}^{-1}$  is assumed, unless otherwise specified.

**Table 1.** BeppoSAX observations log.  $T_{\text{exp}}$  and CR are the total effective exposure time and count rate in the 0.1–2 keV, 2–10 keV, and 15–200 keV energy ranges for the LECS, MECS, and PDS, respectively.

Source	$T_{\text{exp}}^{\text{LECS}}$ (ks)	$\text{CR}^{\text{LECS}}$ ( $\text{s}^{-1}$ )	$T_{\text{exp}}^{\text{MECS}}$ (ks)	$\text{CR}^{\text{MECS}}$ ( $\text{s}^{-1}$ )	$T_{\text{exp}}^{\text{PDS}}$ (ks)	$\text{CR}^{\text{PDS}}$ ( $\text{s}^{-1}$ )
Nov. 96	16.4	$(3.40 \pm 0.16) \times 10^{-2}$	55.7	$0.375 \pm 0.03$	41.5	$0.78 \pm 0.05$
Mar. 97	16.6	$0.130 \pm 0.003$	45.7	$0.697 \pm 0.004$	53.8	$1.05 \pm 0.05$

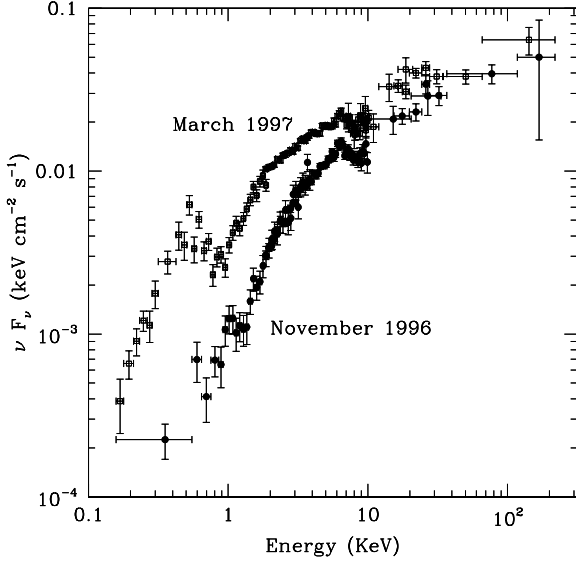


**Figure 1.** X-ray Spectral Energy Distribution for the NGC 3516 BeppoSAX observations of 1996 November (filled circles) and 1997 March (empty squares).

### 3 THE NGC 3516 SPECTRAL ENERGY DISTRIBUTION

Inspection of Tab. 1 suggests that a dramatic spectral change occurred between the two BeppoSAX observations. The 0.1–2 keV:2–10 keV:15–20 keV count rate ratios were 0.04:0.48:1 and 0.12:0.67:1 in 1996 November and 1997 March, respectively, suggesting a much softer source in the second observation. This is more quantitatively shown in Fig. 1, where the X-ray Spectral Energy Distributions (SED) measured by BeppoSAX are compared. The 1996 November SED was fainter in the whole 0.1–50 keV energy range, and significantly harder. In contrast, the 1997 March spectrum exhibits a deep absorption structure, starting at  $\approx 0.7$  keV. A similar structure, if present in 1996 November, is much less pronounced. The effect is even more clearly displayed in Fig. 2, where the 1997 March versus 1996 November LECS/MECS spectral ratio is presented. It increases dramatically for  $E \lesssim 5$  keV. A deep depression in the ratio between 0.7 and 1 keV suggests the presence of a localized absorption feature in the second spectrum which is absent, or much less pronounced, in the earlier one.

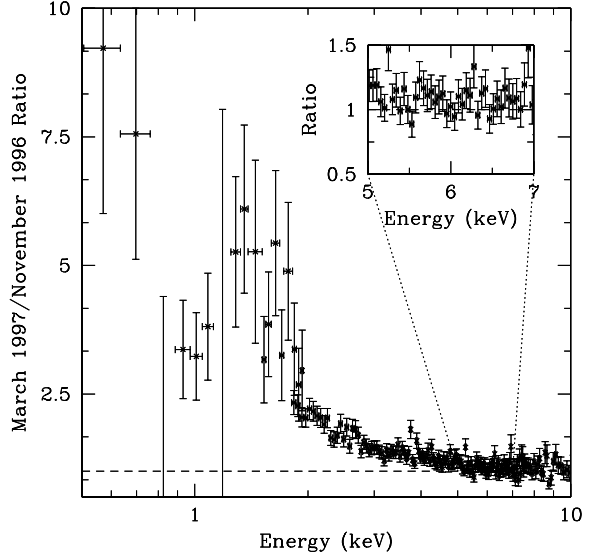


**Figure 2.** LECS ( $E < 2$  keV) and MECS ( $E \geq 2$  keV) spectral ratio between the BeppoSAX NGC 3516 1997 March and 1996 November observations. The inset shows a blow-up of the ratio in the 5–7 keV band.

### 4 SPECTRAL ANALYSIS

No significant spectral variability was found during either BeppoSAX observation, *e.g.* between the 0.5–1.5 keV and 2–10 keV energy ranges (in the former the contribution of the warm absorber to the flux changes is the strongest). We therefore in this section focus on the time-averaged spectra only, measured separately during the two observations.

The ASCA Solid Imaging Spectrometer (SIS; Gen-dreau 1995) has a better energy resolution than the BeppoSAX instruments in the overlapping energy band (0.5–10 keV). Therefore, ASCA results may represent a valuable “pathfinder” for a proper modeling of the BeppoSAX spectra, especially for narrow-band features such as lines and absorption edges. NGC 3516 has been observed several times by ASCA, and the results are discussed in various papers (Kriss et al. 1996; Reynolds 1997; George et al. 1998a; Nandra et al. 1999). All the above papers agree on a “base-line” spectral model, whose main ingredients are: a) a flat  $\Gamma \simeq 1.7$  (this results is, however, challenged by George et al. 1998a) power-law continuum; b) a relativistic iron  $K_{\alpha}$  fluorescent emission line; c) a warm absorber. The contribution of the cold photoelectric absorption due to our Galaxy is generally well accounted for by a fixed column density  $N_{\text{H,Gal}} = 3 \times 10^{20} \text{ cm}^{-2}$ .

Time-averaged spectra were created from cleaned event

file lists, extracted from the ASCA public archive. The data reduction followed standard criteria, as in Nandra et al. (1997a), except for the spectral rebinning, which followed the recipe given in Sect. 2. We could basically reproduce the main results presented by the above authors and we will not include the results of this reanalysis here for simplicity (note, however, that we use our own results when describing the properties of the ASCA observations in Sect. 5).

Given the much wider energy coverage of BeppoSAX, the baseline model defined for ASCA is not appropriate. Following the approaches of Guainazzi et al. (1999) and Perola et al. (1999), a Compton-reflection component (model **pexrav** in XSPEC; Magdziarz & Zdziarski 1995) was included in the baseline model. The relative normalization  $R$  between the reflected and the transmitted continua (equal to 1 for reflection of an isotropically emitted primary continuum by a plane-parallel infinite slab) and the intrinsic cut-off energy  $E_c$  of the primary continuum were allowed to vary. In order not to overfit the BeppoSAX data other reflection model parameters were held fixed at physically meaningful values. The disk inclination was fixed to the value derived from the long-look 1999 ASCA observation ( $35^\circ$ ; Nandra et al. 1999), assuming that the iron line is produced in an X-ray illuminated relativistic disk (model **diskline** in XSPEC, Fabian et al 1989). Solar abundances were assumed throughout. Finally, we assumed that the iron line emitting region extends to the innermost stable orbit around a Schwarzschild black hole, and a radial emissivity parameter  $q = -2$  (Nandra et al. 1997a).

We have chosen a simple parameterization of the warm absorber with individual absorption edges, for ease of comparison with previous works. We have then added edges individually to the fit until statistically required at a confidence level  $>99\%$ , according to the F-test.

This modified baseline model (“BeppoSAX baseline” hereafter) provides an acceptable fit to the 1997 March BeppoSAX time-averaged spectrum with a  $\chi^2$  of 328.5 for 284 degrees of freedom (dof; see Tab. 2), and the corresponding residuals are quite smooth (see Fig. 3). Three edges are required, whose threshold energies are consistent, within the statistical uncertainties, with  $K\alpha$  photoionization from O VII ( $E_{th} = 0.737$  keV), O VIII ( $E_{th} = 0.871$  keV) and FeXV–XIX.

The situation in the 1996 November spectrum is much more complex. In Fig. 4, the LECS residuals against a fit with the BeppoSAX baseline model are shown, where the energy thresholds of the absorption edges below 1 keV were held fixed at their physical values in the source rest frame. The fit quality is poor, and line- or edge-like features are evident. Formally, an excellent fit is obtained if the edge energies are left free in the fit ( $\chi^2_\nu \simeq 0.92$ ; model “B” in Tabs. 3 and 4). In this case the best-fit values are now  $E \simeq 0.67$  keV and  $E \simeq 1.17$  keV. Alternatively, good fits are obtained keeping the edge threshold energies fixed at the O VII and O VIII values and adding an unresolved Gaussian emission line (model “B+G” in Tabs. 3 and 4;  $\chi^2_\nu \simeq 0.93$ ) or a blackbody component (model “B+B” in Tabs. 3 and 4;  $\chi^2_\nu \simeq 0.92$ ). All the above models have problems, which make them physically implausible, or not self-consistent. We discuss the implications of these results in Sect. 5. In general, we find a very hard intrinsic spectrum ( $\Gamma \simeq 1.3$ ) - and, correspondingly, very low values of  $E_c$  ( $\simeq 30$  keV) and  $R$  ( $\lesssim 0.3$ ) - and a surprisingly large soft X-ray line with an

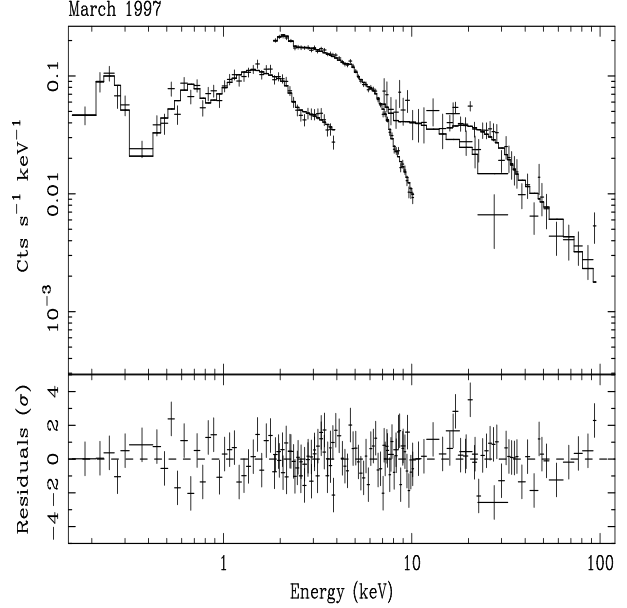


**Figure 3.** Spectra (*upper panel*) and residuals in units of standard deviations (*lower panels*), when the BeppoSAX baseline model is applied to the time-averaged BeppoSAX spectra of the 1997 March observation.

EW of  $\simeq 1.8$  keV, or blackbody fluxes. Moreover, all models require a substantial “cold” photoelectric column of  $0.2\text{--}1.1 \times 10^{22} \text{ cm}^{-2}$ .

A much simpler, elegant and self-consistent solution is to substitute the warm with a cold absorber, and allow its covering fraction to be a free parameter. The fit quality is again excellent ( $\chi^2_\nu = 0.92$ ) and the residuals unstructured (see Fig. 5). In this framework, the properties of the intrinsic nuclear spectrum are very similar during the two BeppoSAX observations (cf. Tab. 2 and Tab. 3). The inferred *cold* column density ( $N_H \simeq 2 \times 10^{22} \text{ cm}^{-2}$ ), is more than two orders of magnitude higher than measured in any other ROSAT, ASCA or BeppoSAX observation, and its covering fraction  $>80\%$ . If absorption edges from O VII, O VIII or ionized iron (with  $E_{th} = 7.7$  keV) are added to the model, only upper limits are obtained with optical depths, of 1.0, 0.2 and 0.4, respectively. The 90% upper limit on the ionization parameter  $\xi^*$  of the cold absorbing matter is 1.6, assuming  $T = 2 \times 10^5$  K. In Fig. 6 we show the column density versus spectral index  $\text{iso-}\chi^2$  contour plot. At the 99% confidence level for two interesting parameters,  $N_H$  is comprised between  $1.4$  and  $2.4 \times 10^{22} \text{ cm}^{-2}$ . We consider the “partial covering” scenario the most plausible model for the 1996 November BeppoSAX time-averaged spectrum, and will discuss its properties in the remainder of this section.

We note that the “warm” and “neutral partial covering” scenarios for the absorber are not mutually interchangeable. The latter scenario yields a  $\chi^2 = 364.1/288$  dof if applied to the 1997 March data. This conclusion applies *a fortiori*

\*  $\xi \equiv L/nR^2$ , where  $L$  is the integrated luminosity of the nuclear source in the 5 eV–300 keV energy range (Done et al. 1992),  $n$  is the plasma electron density and  $R$  its distance from the illuminating source

**Table 2.** Best-fit parameters when the BeppoSAX baseline model (see Sect. 4) is applied to the 1997 March time-average spectrum. The quantities with the subscript  $i$  represent the photoionization absorption edges quantities

$N_H^a$	$\Gamma$	$E_{Fe}^b$ (keV)	$\log(R_o)^c$	$EW_{Fe}^d$ (eV)	$E_1$ (keV)	$\tau_1$	$E_2$ (keV)	$\tau_2$	$E_3$ (keV)	$\tau_3$
$4 \pm 2$	$1.60 \pm 0.03$	$6.52 \pm_{0.48}^{0.13}$	$0.78 \pm_{0.01}^{0.04}$	$170 \pm_{90}^{100}$	$0.71 \pm 0.03$	$1.4 \pm_{0.7}^{0.5}$	$0.91 \pm 0.07$	$0.5 \pm_{0.4}^{0.7}$	$7.73 \pm_{0.17}^{0.19}$	$0.30 \pm_{0.08}^{0.09}$

<sup>a</sup>in units of  $10^{20} \text{ cm}^{-2}$

<sup>b</sup>rest-frame photon energy of the relativistic line

<sup>c</sup>logarithm of the outer radius of the iron line photon emitting region (expressed in units of gravitational radii)

<sup>d</sup>iron line equivalent width

**Table 3.** Best-fit parameters and results for the continuum and iron line components in the BeppoSAX NGC 3516 1996 November observation. Description of the models: B = BeppoSAX baseline; B+G = BeppoSAX baseline with unresolved soft X-ray emission line; B+B = BeppoSAX baseline plus blackbody; PC = partial covering (more details in text). The values for the absorption edges and additional soft X-ray component in models “B”, “B+G” and “B+B” are reported in Tab. 4

Model	$N_H^a$	$C_f^b$ (%)	$\Gamma$	$E_L^c$ (keV)	$\log(R_o)^d$	$EW^e$ (eV)	$\chi^2/\text{dof}$
B	$18 \pm 4$	$100^f$	$1.32 \pm_{0.16}^{0.14}$	$6.46 \pm 0.14$	$< 1.3$	$300 \pm 20$	250.5/272
B+G	$27 \pm_{10}^{13}$	$100^f$	$1.28 \pm 0.12$	$6.4 \pm 0.2$	$< 1.1$	$310 \pm 120$	257.4/273
B+B	$140 \pm 20$	$100^f$	$1.46 \pm 0.17$	$6.4 \pm_{0.3}^{1.1}$	$< 1.2$	$330 \pm 140$	246.7/273
PC	$210 \pm_{20}^{30}$	$84 \pm 4$	$1.53 \pm_{0.09}^{0.11}$	$6.5 \pm 0.3$	$> 0.84$	$290 \pm 120$	240.2/271

<sup>a</sup>in units of  $10^{20} \text{ cm}^{-2}$

<sup>b</sup>covering fraction of the cold photoelectric absorber

<sup>c</sup>rest-frame photon energy of the relativistic line

<sup>d</sup>logarithm of the outer radius of the iron line photon emitting region (expressed in units of gravitational radii)

<sup>e</sup>iron line equivalent width

<sup>f</sup>fixed

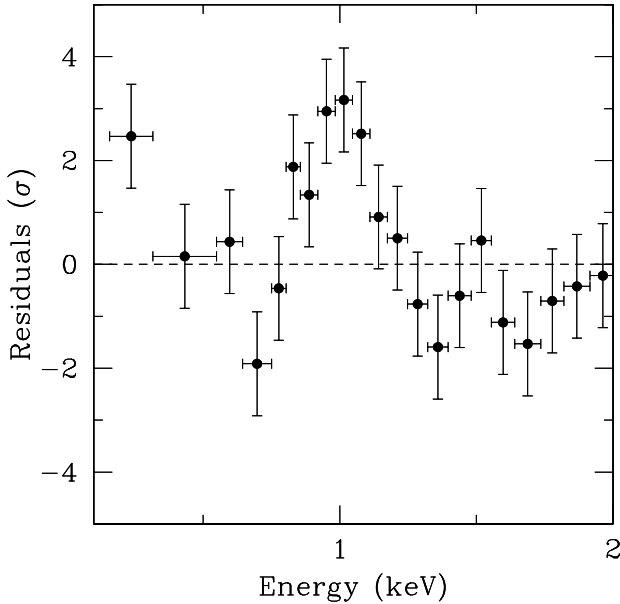


**Figure 4.** LECS residuals in units of standard deviations below 2 keV, when the best-fit baseline model is applied to the 1996 November BeppoSAX spectrum, once the O VII and O VIII absorption edges threshold energies are fixed at their physical values in the source rest frame.

to the ASCA observations. The  $\chi^2$  is 573.1 for 532 dof and 640.6 for 539 dof for the former scenario in the 1994 April and 1995 March observations (our reanalysis), whereas it is 1647/547 dof and 950.6/544 dof in the latter, respectively.

The BeppoSAX results confirm that the spectral index

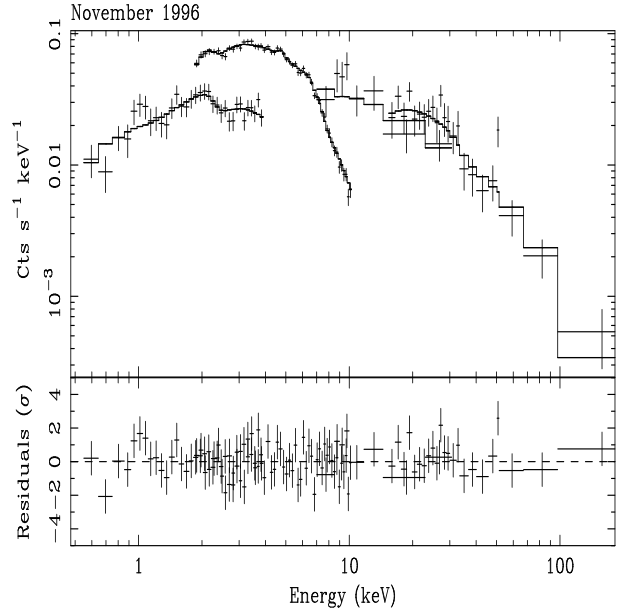


**Figure 5.** Spectra (*upper panel*) and residuals in units of standard deviations (*lower panel*), when the model with partial covering neutral photoelectric absorption is applied to the time-averaged BeppoSAX spectra of the 1996 November observation.

of the primary continuum in NGC 3516 ( $\Gamma \simeq 1.5$ ) is flatter than typically observed in Seyfert galaxies (Nandra et al. 1997), albeit not extreme. In Tab. 5 the best fit values for  $R$  and  $E_c$  are shown. Despite a factor  $>1.5$  increase of the 0.5–10 keV flux between the two BeppoSAX observations, both quantities remain constant, in agreement with the disk reflection paradigm.

**Table 4.** Best-fit parameters and results for the absorption edges and additional soft X-ray component (rows 2 and 3 only) in the BeppoSAX NGC 3516 1996 November observation. The other parameters are reported in Tab. 3. The labeling of the models is the same as in Tab. 3

Model	$E_1$ (keV)	$\tau_1$	$E_2$ (keV)	$\tau_2$	$E_3$ (keV)	$\tau_3$	$E_L^b/kT^c$ (keV)/(eV)	$EW_L^d$ (keV)
B	$0.67 \pm_{0.08}^{0.10}$	$2.5 \pm 0.6$	$1.17 \pm 0.06$	$1.79 \pm_{0.10}^{0.19}$	$7.7 \pm_{0.3}^{0.2}$	$0.36 \pm 0.06$		
B+G	$0.737^a$	$< 2.6$	$0.871^a$	$4.2 \pm_{1.5}^{0.9}$	$7.7 \pm_{0.2}^{0.3}$	$0.38 \pm_{0.09}^{0.12}$	$1.06 \pm_{0.05}^{0.02}$	$1.8 \pm_{0.8}^{1.0}$
B+B	$0.737^a$	$2.3 \pm 1.2$	$0.871^a$	$< 0.7$	$7.8 \pm 0.3$	$0.30 \pm_{0.10}^{0.08}$	$74 \pm_7^5$	

<sup>a</sup>fixed  
<sup>b</sup>centroid energy of the soft X-ray Gaussian line  
<sup>c</sup>temperature of the blackbody component  
<sup>d</sup>EW of the soft X-ray Gaussian line

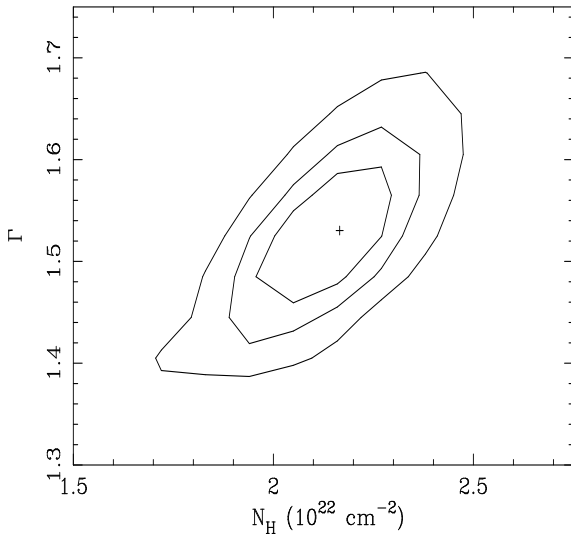


**Figure 6.** Column density versus spectral index iso- $\chi^2$  contour plot for the “PC” model applied to the November 1996 BeppoSAX spectra. The contours represent the 68%, 90% and 99% confidence levels for two interesting parameters

**Table 5.** Best-fit Compton-reflection versus primary continuum relative normalization (R) and cut-off energy ( $E_c$ ) in the two BeppoSAX observations.

Date	R	$E_c$ (keV)
1996 November	$0.7 \pm_{0.4}^{0.5}$	$140 \pm_{60}^{220}$
1997 March	$0.7 \pm_{0.3}^{0.4}$	$120 \pm_{40}^{80}$

The best-fit models correspond in the 1996 November (1997 April) observation to observed fluxes of 0.27 (1.36) and  $2.50$  ( $4.41$ )  $\times 10^{-11}$  erg cm $^{-2}$  s $^{-1}$  in the 0.5–2 keV and 2–10 keV energy bands, respectively. These values correspond to unabsorbed rest-frame luminosities of 0.43 (0.71) and  $1.01$  ( $1.56$ )  $\times 10^{43}$  erg s $^{-1}$ , respectively.

## 5 DISCUSSION

We compare the time-averaged spectra of NGC 3516 measured by BeppoSAX during two observations separated by four months. The earlier spectrum is weaker and harder in the whole 0.1–50 keV energy range. In addition, the deep

absorption edges from ionized oxygen, which have been observed by ROSAT (Mathur et al. 1997) and ASCA (Kriss et al. 1996; Reynolds 1997; George et al. 1998a) are much less pronounced. These remarkable spectral changes could in principle reflect a dramatic modification either of the condition of the cold/warm photoelectric absorption, or of the mechanism producing the primary nuclear continuum.

We propose that these changes are most easily interpreted as due to the onset of substantial cold absorption ( $N_H \simeq 2 \times 10^{22}$  cm $^{-2}$ ) along the line of sight to the nucleus during the earlier observation. The properties of the primary continuum and of the Compton reflection components do not appear to have substantially changed between the two observations, despite an overall increase of the 2–10 keV flux by a factor about 1.5.

### 5.1 NGC3516: a low-luminosity BAL quasar?

This is not the first claim that the nucleus of NGC 3516 is seen through a substantial “cold” column density. The same conclusion was reached by Kruper et al. (1990), on the basis of *Einstein* MPC observations and by Ghosh & Soundararajaperumal (1991) using EXOSAT. A 1989 *Ginga* spectrum also required a column density of  $N_H \simeq 4 \times 10^{22}$  cm $^{-2}$  (Kolman et al. 1993). However, in all subsequent ROSAT and ASCA observations, NGC 3516 turned out to be a “standard” warm absorbed Seyfert 1. This casts doubt on the previous interpretations, which were obtained using less sensitive instruments. The BeppoSAX finding is the first confirmation with moderate resolution detectors that NGC 3516 indeed undergoes phases with large amounts of absorption by cold material.

It is difficult, currently, to unambiguously characterize the physics and/or geometry underlying these changes. We investigate two main options in the following: *i*): the cold absorber constitutes a different absorbing system from the warm absorber; *ii*) the observed variability reflects changes in the physical properties of the warm absorber itself.

The former scenario can be simply described as the interposition of “bricks” of matter, with  $N_H \sim 10^{22}$ – $10^{23}$  cm $^{-2}$ , along the line of sight to the nucleus. The available observations have a too sparse a pattern to provide any strong quantitative constraints on the nature of these “bricks”. It is likely that there are a small number of big clouds, because it is difficult to reproduce simultaneously the apparent “on-off” pattern of high absorption occurrences (from null to  $\gtrsim 10^{22}$  cm $^{-2}$ ) and the lack of significant spectral variability within an observation of typical

duration a few days with a large number of randomly distributed clouds. The properties of the absorbing cloud(s) can be constrained, using the limits on the variability timescales available from the BeppoSAX observations (*i.e.*: minimum of 1 day - the length of the November 1996 observation - and maximum of 4 months - the distance between the two observations), and the upper limit on the ionization parameter of the absorbing matter ( $\xi < 1.6$ ). Assuming a single spherical cloud of radius  $r$  rotating with Keplerian velocity  $v_K$  around a black hole of mass  $M_6 = M_{BH}/10^6 M_\odot$ :

$$v_K = \left(\frac{GM_{BH}}{R}\right)^{1/2} = \left(\frac{\xi N_H}{Lr}\right)^{1/4} (GM_{BH})^{1/2}$$

The “disappearance” of the cold absorber in the April 1997 observation implies  $r/v_K \lesssim 10^7$  s, or:

$$r^{5/4} < 4 \times 10^{26} N_H^{1/4} L^{-1/4} (GM_6)^{1/2} \simeq 6 \times 10^{17} \text{ cm}^{5/4}$$

or  $r < 6 \times 10^{14}$  cm ( $L = 6 \times 10^{43}$  erg s $^{-1}$  in the November 1996 observation). The lower limit on the distance between the absorbing cloud and the nuclear illuminating source can be expressed (again through the ionization parameter definition) as  $R > 2 \times 10^{17} n_9^{-1/2}$ , ( $n_9$  is the electron density in units of  $10^9$  cm $^{-3}$ ). Given the above constraints, it is interesting to test the hypothesis whether the absorbing matter is associated with the Broad Line Regions (BLR). We assume the measured FWHM of the  $H_\beta$  line (4000 km s $^{-1}$ ; Wanders et al. 1993) as the velocity of the cloud. The size of the cloud is therefore constrained in the range  $4 \times 10^{13} \lesssim r \lesssim 4 \times 10^{15}$  cm, corresponding (through  $N_H \equiv nr$ ) to a range in electron densities:  $5 \times 10^6 \lesssim n < 5 \times 10^8$  cm $^{-3}$ . This range is only marginally consistent with the current estimates of the characteristic densities in BLR ( $n \sim 10^9$ – $10^{12}$  cm $^{-3}$ ; see *e.g.* Krolik et al. 1991). Moreover, our lower limit on  $R$  is not consistent with the reverberation mapping measurements of the BLR size ( $\sim 3 \times 10^{16}$  cm; Wanders et al. 1993), unless *high* densities are assumed.

The Broad Absorption Lines quasars (BALs) are a class of quasars, characterized by strong high-ionization absorbing features. The UV absorbing system in NGC 3516 (Voit et al. 1987; Walter et al. 1990) strongly resembles those of BALs. There are, however, significant differences, namely the lower EW ( $\sim 40\text{\AA}$  in BALs versus  $\lesssim 10\text{\AA}$  in NGC 3516), the range in velocity (up to 10000 km s $^{-1}$  versus 3000 km s $^{-1}$ ) and the variability timescales (years versus weeks/months). Kolman et al. (1993) were the first to speculate that NGC 3516 may be a low-redshift counterpart of the BALs, and its peculiar properties may be mainly due to the weaker nuclear engine energy output. The variability timescale of the UV absorption features is of the same order as the (most likely) occurrence of the high X-ray absorption states. Intriguingly, recent studies of a sample of BAL quasars using ROSAT, ASCA and BeppoSAX (Gallagher et al. 1999; Brandt et al. 1999) discovered that they are considerably weaker X-ray sources than expected from their optical fluxes, and column densities as high as several  $10^{23}$  cm $^{-2}$  are not uncommon. We can extend the original speculation further and propose that the X-ray highly absorbed states in NGC 3516 are connected to the onset of UV absorption features. In the cases where simultaneous UV/X-ray data are available, this connection is indeed present (Kolman et al. 1993; Koraktar et al. 1996; Kriss et al. 1996). Weymann

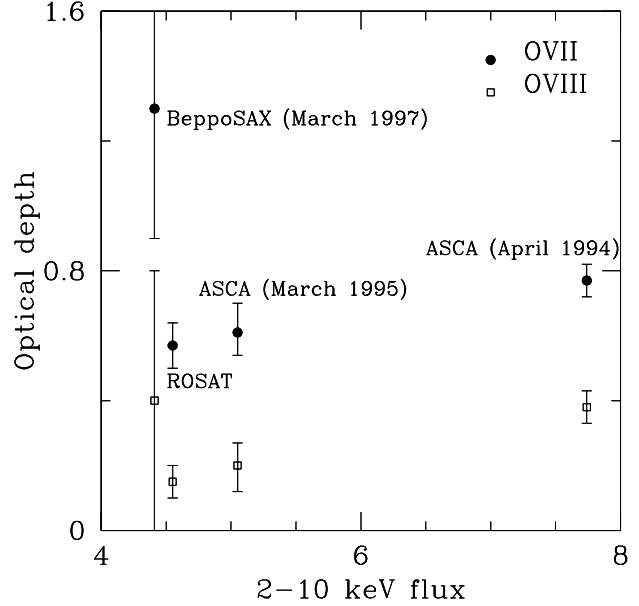


**Figure 7.** Best-fit absorption edges optical depths against 2–10 keV flux in ROSAT (Mathur et al. 1997), ASCA (our reanalysis) and BeppoSAX 1996 April (this *paper*) time-averaged spectra for O VII (filled circles) and O VIII (empty squares). The flux for the ROSAT observation is extrapolated from the best-fit warm absorber model of Mathur et al. (1997). In all cases the baseline model defined in Sect. 4 is used (Compton reflection included for BeppoSAX data only), with the threshold energies of the edges fixed at their physical values in the source rest frame.

et al. (1991) suggested that the clouds responsible for the BAL phenomenon are ablated from the rim of the molecular torus surrounding the nuclear region of the AGN. Intriguingly, the velocity field of the circum-nuclear emission-line regions suggests that our line of sight towards the NGC 3516 nucleus indeed grazes the putative torus (Goad & Gallagher 1987). However there are still theoretical difficulties in encompassing the cold X-ray and UV absorption features in one and the same absorbing system. As pointed out by Kolman et al. (1993), it is difficult to obtain the observed width of the C IV absorption feature with a column density of the order of  $10^{22}$  cm $^{-2}$ .

## 5.2 A “non-standard” warm absorber?

Alternatively, these intervals of apparent high “cold” absorption could be due to a change in the physical properties (namely the ionization structure) of the warm absorber itself. A comparison of the measured O VII and O VIII absorption edge optical depths with the 2–10 keV flux before BeppoSAX shows, if any, a slight trend for both edges to become deeper with increasing flux (Fig. 7), which would exclude simple models, where the equilibrium ionization structure of the absorber is mainly driven by the average ionizing continuum. Mathur et al. (1997) developed a dynamical model to explain the changing features of the UV and X-ray absorber (“XUV system”). According to their model, the XUV system is outflowing with a radial velocity of  $\simeq 500$  km s $^{-1}$ .

The disappearance of the UV absorption lines is due to an increase of the ionization parameter caused by the decreasing density in the expanding matter. They predicted a progressive weakening of the O VII edge in comparison to the O VIII. Ultimately, the absorber would become totally transparent to X-rays. This prediction is not fulfilled by the BeppoSAX observations presented here. The 1997 April spectrum is well fit within the framework of a “standard” warm absorber scenario, and the O VII absorption edge optical depth is almost double the maximum observed by ROSAT (Mathur et al. 1997) and ASCA (Kriss et al. 1996; Reynolds 1997; our re-analysis of archival data; see Fig. 7). A new absorbing system must have been produced in the meanwhile.

Another question is whether differing conditions of the warm absorber can *mimic* a substantial neutral column density in instruments with moderate energy resolution such as those on BeppoSAX. Actually, the 1996 November spectrum can be formally well fit within a warm absorber framework, where the opacity is described by two absorption edges of  $\simeq 0.67$  and  $\simeq 1.17$  keV. The recent discovery of the so-called “1 keV” warm absorber features in the X-ray spectrum of some Narrow Line Seyfert 1 Galaxies (Leighly et al. 1997) has raised new interest and theoretical speculations on this subject. Nicastro et al. (1999a, 1999b) demonstrate that strong absorption features in the range 1–3 keV can be produced under two different physical conditions: a) if the ionizing continuum is steeper than observed in “broad” Seyfert 1 galaxies; b) or - and this is the scenario which may be relevant to our case - if collisional ionization dominates. In the latter scenario, the highest source of opacity is provided by ionized species of neon and iron (L-transitions). However, this explanation presents several problems. The first is that the 0.67 keV feature has an energy appropriate to O VI (Lithium-like oxygen), which only dominates the ionic distribution for a narrow range of ionizing fluxes. Similar considerations apply if the feature is instead identified with N VII. However, the observed feature is not formally inconsistent, within the statistical uncertainties, with the more common  $K_{\alpha}$  photoionization from O VII. The 1.17 keV feature can be associated with either Ne IX or Fe XVII–XVIII. A range of electron temperatures around a few  $10^6$  K exist, where these species have simultaneously the highest relative fractional abundance in a collisionally ionized plasma (Nicastro et al. 1999a). Such high temperatures would be associated with a ionization distribution of oxygen where the contribution of O VIII is important, if not dominant, making the identification of the lower energy edge even more problematic. However, Nicastro et al. (1999a) show that the simultaneous presence of O VII and “1-keV” features can be achieved with mixed collisional-photoionization models, which also predict a decoupling of the ionization parameter of the gas from the ionizing continuum flux. The main obstacle to the viability of this model remains, however, the extremely flat intrinsic power-law spectrum that requires ( $\Gamma \simeq 1.3$ ) - and the correspondingly low cutoff energy ( $E_c \simeq 30$  keV) -, which has never been observed in NGC 3516 or other Seyfert 1 galaxies (Nandra & Pounds 1994; Nandra et al. 1997a). We therefore consider this a very unlikely possibility.

**Table 6.** Best-fit parameters for the ionized iron absorption edge in the ASCA and March 1997 BeppoSAX observations. The  $\Delta\chi^2$  refers to the addition of this feature to the model (corresponding to 2 less dofs). The best-fit model is the baseline (without Compton reflection for the ASCA observations)

Date	$E_{th}$	$\tau$	$\Delta\chi^2$
1994 April <sup>a</sup>	$7.75 \pm 0.17$	$0.27 \pm_{-0.06}^{+0.07}$	57
1995 March <sup>a</sup>	$7.7 \pm 0.3$	$0.27 \pm_{-0.12}^{+0.10}$	8.3
1997 March <sup>b</sup>	$7.73 \pm_{-0.17}^{+0.19}$	$0.30 \pm_{-0.08}^{+0.09}$	37

<sup>a</sup>ASCA

<sup>b</sup>BeppoSAX

### 5.3 The iron edge problem

The 1997 March BeppoSAX observation baseline best-fit model requires an absorption edge, whose threshold energy (7.7 keV) corresponds to  $K_{\alpha}$  photoionization from highly ionized iron (FeXV–XIX). It is very unlikely that the oxygen and the iron absorption features originate in the same warm absorber. If we assume the photoionization cross sections of Verner & Yakovlev (1995) and the abundances of Anders & Grevesse (1989), the hydrogen equivalent column densities for oxygen and iron differ by more than one order of magnitude:  $N_O^H \sim 1.2 \times 10^{21} \text{ cm}^{-2}$ ,  $N_{Fe}^H \sim 3 \times 10^{22} \text{ cm}^{-2}$ . The iron feature is at 20% of the best-fit continuum/data ratio, then significantly deeper than any reported calibration uncertainties in the MECS at those energies ( $\simeq 5\%$ ; Fiore et al. 1999). Moreover, analogous features are detected in the publicly available ASCA spectra. In Tab. 6 we report the best-fit threshold energy and optical depth of this feature in the ASCA observations, when the baseline model (without Compton reflection) is applied (the 1997 March BeppoSAX measurement is also reported for ease of comparison). The ASCA and BeppoSAX measures are very consistent. We note in passing the the upper limit on the optical depth of a 7.7 keV absorption edge (0.4) in the BeppoSAX 1996 September observation is also consistent with these values. In principle, a strong iron overabundance in the absorbing medium could reconcile the discrepancy. A contribution to the iron absorption edge could come from the opacity in a partly ionized reflector. However, the latter hypothesis is contradicted by the fact the the iron line measured by ASCA (Nandra et al. 1999) is inconsistent with being produced by fluorescence of significantly ionized iron. Alternatively, the iron edge could originate in a second warm absorber, more ionized than that responsible for the oxygen features. We have investigated this possibility, fitting the April 1997 BeppoSAX spectrum with a double ionized absorber model. We have assumed two scenarios: either the primary continuum reaches us through a single optical path, along which the two absorbing screens are located; or it follows two different optical paths, and one absorbing screen is located along each of them. The XSPEC implementation `absori` for the warm absorber has been used in these fits. The best-fit parameters and results are summarized in Tab. 7. The quality of these fits is comparable with the phenomenological fits in Sect. 4. However, they suffer a serious inconsistency. They require a steep intrinsic spectrum ( $\Gamma \simeq 2.1$ ), and a correspondingly larger amount of reflection ( $R = 2\text{--}3$ ). On the other hand, the iron line EW is very small ( $\simeq 60\text{--}100$  eV). This is inconsistent with the disk paradigm (Matt et al. 1992), unless



**Table 7.** Best-fit parameters and results when the double ionized absorption model is applied to the BeppoSAX April 1997 observation. The rows correspond to either one of the following scenarios: a model where the absorbing screens are located along the same optical path (row 1); the absorbing screened are located along different optical paths (row 2)

First absorber			Second absorber			Continuum		Iron line		$\chi^2/\text{dof}$
$N_{\text{H},1}$ ( $10^{22} \text{ cm}^{-2}$ )	$\log(\xi_1)$	$\log(T_1)$	$N_{\text{H},2}$ ( $10^{22} \text{ cm}^{-2}$ )	$\log(\xi_2)$	$\log(T_2)$	$\Gamma$	R	E (keV)	EW (eV)	
$1.17 \pm_{-0.13}^{+0.17}$	$0.2 \pm_{-0.7}^{+0.2}$	$6.7 \pm 0.6$	$9 \pm_4^6$	$2.6 \pm_{-1.0}^{+0.5}$	$\equiv T_1$	$2.06 \pm_{-0.05}^{+0.08}$	$2.1 \pm_{-0.6}^{+1.0}$	$6.3 \pm 0.2$	$100 \pm_{70}^{+90}$	334.8/287
$0.57 \pm_{-0.05}^{+0.08}$	$< 0.17$	$5.7 \pm_{-0.4}^{+1.5}$	$4.6 \pm_{-0.8}^{+2.4}$	$1.9 \pm_{-1.3}^{+2.1}$	$< 5.9$	$2.15 \pm_{-0.06}^{+0.03}$	$3.0 \pm_{-0.4}^{+1.3}$	$6.3 \pm 0.2$	$60 \pm_{30}^{+40}$	342.4/286

the line is significantly ionized (Matt et al. 1993; Życki et al. 1994). Again, this hypothesis is, however, not supported by the observational evidence available so far.

#### 5.4 NGC3516 in hard X-rays: a reassuring “standard” Seyfert 1

The other X-ray spectral features of NGC3516 are not uncommon among Seyfert 1 galaxies. The intrinsic spectral index measured by BeppoSAX is flat ( $\Gamma \simeq 1.6$ ), but not extreme. The Compton reflection is slightly smaller, but not inconsistent, with a that expected from a plane-parallel slab subtending a  $2\pi$  angle from the nucleus (*i.e.* an accretion disk). The iron line EW is consistent, within the statistical uncertainties, to having an origin in the same accretion disk [this would *not* be the case for the line EW measured by ASCA (Nandra et al. 1997b; Nandra et al. 1999), suggesting long-term changes in the relative weights of the reprocessed components]. It is worth noting the constancy of the amount of Compton reflection between the two BeppoSAX observations, despite a 1.5 variation in the 2–10 keV luminosity. This allows an upper limit on the size of the reflecting region of about 0.1 pc to be set. It is likely to be smaller than this. The study of the intra-observation (*i.e.* intra-day) variability pattern, is consistent with a response of the Compton reflection on timescales as short as a few thousand seconds. Similar conclusions were reached by Nandra et al. (1997b) from their study of the iron line flux variability in the ASCA observations.

After the present work was completed, we became aware of a paper discussing the same set of data by Costantini et al. (2000). Although their main conclusions coincide with ours, they report the detection of the ionized iron absorption edge also in the November 1996 observation (due to the different parameterization used, it is not straightforward to compare their detection with our upper limit). They attribute it to a “highly photoionized component [...], mainly visible when our view of the primary X-rays is at least partially covered by a large amount of neutral absorber”. Moreover, their fits yield a steeper intrinsic spectral index ( $\Gamma = 2$ ), with a correspondingly larger amount of reflection ( $R \simeq 1.2$ – $1.4$ ).

#### ACKNOWLEDGMENTS

The BeppoSAX satellite is a joint Italian-Dutch programme. M. Guainazzi acknowledges an ESA Fellowship and W. Marshall the ESA stagiare programme. This research has made use of data obtained through the High Energy Astrophysics

Science Archive Research Center Online Service, provided by the NASA/Goddard Space Flight Center.

#### REFERENCES

- Anders E., Grevesse N., 1989, *Geochimica and Cosmochimica Acta*, 53, 197
- Antonucci R. R. J., Miller J. S., 1985, *ApJ*, 297, 621
- Antonucci R. R. J., 1993, *ARA&A*, 31, 473
- Boella G., Butler R. C., Perola G. C., Piro L., Scarsi L., Bleeker J., 1997a, *A&AS*, 122, 299
- Boella G., et al., 1997b, *A&AS*, 122, 327
- Boller Th., Brandt W. N., Fabian A. C., Fink H. H., 1997, *MNRAS*, 289, 393
- Brandt W. N., Gallagher S. C., Laor A., Wills B. J., 2000, *Astroph. Lett. & Comm* in press (astroph/9910302)
- Costantini E., et al., 2000, *ApJ*, in press (astroph/0007158)
- Done C., Mulchaey J.S., Mushotzky R.F., Arnaud K.A., 1992, *ApJ*, 395, 275
- Fabian A. C., et al., 1994, *PASJ*, 46, L59
- Fabian A. C., Rees M. J., Stella L., White N. E., 1989, *MNRAS*, 238, 729
- Fiore F., Guainazzi M., Grandi P., 1999, “A cookbook for BeppoSAX NFI spectral analysis”, SDC-TR
- Frontera F., Costa E., Dal Fiume F., Feroci M., Nicastro L., Orlando M., Palazzi E., Zavattini G., 1997, *A&AS*, 122, 357
- Gallagher S. C., Brandt W. N., Sambruna R. M., Mathur S., Yamasaki N., 1999, *ApJ*, 519, 549
- Gendreau K., 1995, Ph.D Thesis, Massachusetts Institute of Technology
- George I. M., Turner T. J., Mushotzky R. F., Nandra K., Netzer H., 1998b, *ApJ*, 503, 174
- George I. M., Turner T. J., Netzer H., Nandra K., Mushotzky R. F., Yaqoob T., 1998a, *ApJS*, 114, 73
- Ghosh K. K., Soundararajaperumal S., 1991, *ApJ*, 383, 574
- Goad J. W., Gallagher J. S., 1987, *AJ*, 94, 640
- Guainazzi M., et al., 1998, *MNRAS*, 301, L1
- Guainazzi M., Mihara T., Otani C., Matsuoka M., 1996, *PASJ*, 48, 781
- Guainazzi M., Perola G. C., Matt G., Nicastro F., Bassani L., Fiore F., Dal Fiume D., Piro L., 1999, *A&A*, 346, 407
- Keel W.C., 1996, *AJ*, 111, 696
- Kolman M., Halpern J. P., Martin C., Awaki H., Koyama K., 1993, *ApJ*, 403, 592
- Koratkar A., et al., 1996, 470, 378
- Kriss G. A., et al., 1996, *ApJ*, 467, 629
- Krolik J.H., Horne K., Kallmann T.R., Malkan M.A., Edelson R.A., Kriss G.A., 1991, *ApJ*, 371, 541
- Krupe J. S., Canizares C. R., Urry C. M., 1990, *ApJS*, 74, 347
- Laughton M., Margon B., Bowyer S., 1976, *ApJ*, 208, 177
- Leighly K. M., Kay L. E., Mushotzky R. F., Nandra K., Forster K., 1997, *ApJ*, 489, L25
- Manzo G., Giarrusso S., Santangelo A., Ciralli F., Fazio G., Piraino S., Segreto A., 1997, *A&AS*, 122, 341
- Mathur S., Wilkes B. J., Aldcroft T., 1997, *ApJ*, 478, 182

- Matt G., Fabian A.C., Ross R.R., 1993, MNRAS, 262, 179
- Matt G., Perola G.C., Piro L., Stella L., 1992, A&A, 257, 63
- McHardy I. M., Green A. R., Done C., Puchnarewicz E. M., Mason K. O., Branduardi-Raymond G., Jones M. H., 1995, MNRAS, 273, 549
- Mushotzky R. F., 1982, ApJ, 256, 92
- Nandra K., George I. M., Mushotzky R. F., Turner T. J., Yaqoob T., 1997a, ApJ, 476, 70
- Nandra K., George I. M., Mushotzky R. F., Turner T. J., Yaqoob T., 1999, ApJ, 523, L17
- Nandra K., Mushotzky R. F., Yaqoob T., George I. M., Turner T. J., 1997b, MNRAS, 284, L7
- Nandra K., Pounds K., 1994, MNRAS, 268, 405
- Nicastro F., Fiore F., Matt G., 1999b, ApJ, 517, 108
- Nicastro F., Fiore F., Perola G.C., Elvis M., 1999a, ApJ, 512, 136
- Otani C., et al., 1996, PASJ, 48, 211
- Parmar A. N., Martin D. D. E., Bavdaz M., Favata F., Kuulkers E., Vacanti G., Lammers U., Peacock A., Taylor B. G., 1997, A&AS, 122, 309
- Perola G. C., et al., 1999, A&A, 351, 937
- Reynolds C. S., 1997, MNRAS, 286, 513
- Reynolds C. S., Fabian A. C., Nandra K., Inoue H., Kunieda H., Iwasawa K., 1995, MNRAS, 277, 901
- Turner T. J., Pounds K. A., 1989, MNRAS, 240, 883
- Verner D. A., Yakovlev D. G., 1995, A&AS, 109, 125
- Voit G. M., Shull J. M., Begelman M. C., 1987, ApJ, 316, 573
- Walter R., Ulrich M. H., Courvoisier T. J. L., Buson L. M., 1990, A&A, 233, 53
- Wanders I., et al., 1993, A&A, 269, 39
- Weymann R. J., Morris S. L., Foltz C. B., Hewett P. C., 1991, ApJ, 373, 23
- Życki P.T., Czerny B., 1994, MNRAS, 266, 653